

Longitude variations of the solar semidiurnal tides in the mesosphere and lower thermosphere at low latitudes observed from ground and space

Jonathan S. Friedman,¹ Xiaoli Zhang,² Xinzhou Chu,³ and Jeffrey M. Forbes²

Received 16 January 2009; revised 3 April 2009; accepted 8 April 2009; published 10 June 2009.

[1] We present an analysis of longitudinal variation in the solar semidiurnal tide observed in the nocturnal thermal structure of the low-latitude mesopause region (83–103 km), with a focus on two sites: Arecibo, Puerto Rico (18.3°N , 66.8°W) and Maui, Hawaii (20.7°N , 156.3°W). Localized observations made by lidars are combined with longitudinal measurements by Sounding of the Atmosphere using Broadband Emission Radiometry (SABER) and compared with the Global-Scale Wave Model-2002 (GSWM-02) for 6 months: January, April, May, July, August, and October. In winter-spring, lidar-measured amplitudes are larger than those recorded by SABER, whereas in summer the amplitudes are similar and in autumn the lidars observe smaller amplitudes than SABER. GSWM amplitudes are between the lidar and SABER measurements for January, are comparable to the measurements in spring, underpredict for summer, and agree with the lidars in autumn. The phase structure is consistent among lidars and SABER for all of the months except January, when there is a large phase shift, and the local time of the temperature maximum is different between Arecibo and Maui. GSWM shows better agreement with phase measurements in winter-spring than in summer-autumn. Modal analysis of the SABER data indicates that the (2, 2) Hough mode is present throughout the year. In winter, it is joined by the (2, 4) mode, while in summer it is accompanied by the (2, 3) mode. This change in the predominant Hough modes may be related to the winter-summer phase difference.

Citation: Friedman, J. S., X. Zhang, X. Chu, and J. M. Forbes (2009), Longitude variations of the solar semidiurnal tides in the mesosphere and lower thermosphere at low latitudes observed from ground and space, *J. Geophys. Res.*, *114*, D11114, doi:10.1029/2009JD011763.

1. Introduction

[2] The thermal structure of the atmosphere is strongly modulated by solar heating. This produces migrating (Sun-synchronous) tides with periods corresponding to harmonics of a day and amplitudes increasing with altitude. The distribution of landmasses modulates this forcing, as they generate more atmospheric heating than oceans, and this nonuniform forcing results in tidal oscillations that are nonmigrating, i.e., do not follow the Sun. Sun-synchronous, or migrating, atmospheric tides show appreciable amplitudes in the mesosphere and lower thermosphere (MLT) region of the atmosphere. The dominant components are diurnal (24 h) and semidiurnal (12 h), although terdiurnal (8-h) tides are also present [e.g., Chapman and Lindzen, 1970; Forbes, 1995]. Migrating and nonmigrating tides provide a large part of the dynamical forcing that determines

the MLT thermal structure, and they affect the chemical processes related to metallic and other atoms and molecules in the region. MLT tidal variations are observed in temperatures [Chen et al., 2000; Dao et al., 1995; Fricke-Begemann and Höfner, 2005; Salah and Wand, 1974; She et al., 2002, 2004; States and Gardner, 2000b; Taylor et al., 2001; Williams et al., 1998; Yuan et al., 2006, 2008], winds [Roper et al., 1993; She et al., 2002, 2004; Yuan et al., 2006, 2008; Zhou et al., 1997], metal atom densities [Hecht et al., 1998; States and Gardner, 1999; Williams et al., 1998], and airglow intensities [Hecht et al., 1998; Zhang et al., 2001; Zhao et al., 2005].

[3] Tides propagate zonally, so a migrating tide will maximize at the same local time for all longitudes at a fixed altitude and latitude, while nonmigrating effects will show up as longitudinal modulations of amplitude and phase. Observations undertaken at multiple longitudes at a given latitude can help elucidate the dominant modulations, as well as local effects. These observations are generally taken by satellites, though it typically takes many weeks to build a complete local time picture/cycle owing to orbital constraints, and space-based (SB) observations do not provide the continuous local coverage required to see local effects. However, when there are opportunities to make such

¹Arecibo Observatory, NAIC, Arecibo, Puerto Rico, USA.

²Department of Aerospace Engineering Sciences, University of Colorado, Boulder, Colorado, USA.

³CIRES, University of Colorado, Boulder, Colorado, USA.

measurements with multiple ground-based (GB) sites, they can be combined with SB measurements at a given latitude to get a better picture of coherent tidal structure that contains both migrating and nonmigrating tides [Cierpik *et al.*, 2003]. Dominance by migrating tides would be observed as similar tidal structure in local solar time at multiple sites, and SB and GB observations would agree closely, whereas nonmigrating sources can upset this phase and amplitude coherence and can influence the correlation between GB and SB measurements. Although a fixed location site cannot separate multiple oscillations with the same temporal frequency, adding additional locations at the same latitude adds information that helps to make this separation.

[4] Tidal amplitudes also vary with latitude. Hough mode analysis shows that the assortment of modes (diurnal, semidiurnal and higher orders) have distinct latitude variations [Chapman and Lindzen, 1970; Forbes, 1995]. Analysis of SABER measurements has shown that the diurnal tide has consistently small amplitudes near 20°N, sandwiched between equatorial and subtropical ($\sim 30^{\circ}$ latitude) maxima, while the semidiurnal tide has appreciable amplitude for most seasons in the tropics and subtropics [Forbes *et al.*, 2008, Figure 1]. These facts make nocturnal-only observations at 20°N amenable to the zonal 12-h tidal analysis carried out in this report.

[5] The Arecibo Observatory is located at 18.35°N, 66.75°W, and the Maui Space Surveillance Complex is atop Mount Haleakala in Maui, Hawaii at 20.7°N, 156.3°W. These two sites, at similar tropical latitudes and separated by almost 90° in longitude, have hosted Doppler-resonance lidar systems making extensive nocturnal observations of the thermal structure of the upper mesosphere–lower thermosphere [Friedman, 2003; Chu *et al.*, 2005; Friedman and Chu, 2007]. These data sets, recorded between 2002 and 2007, combined with observations by the SABER instrument on board the TIMED satellite [Mertens *et al.*, 2004], give us the opportunity to study the longitudinal variability of the semidiurnal thermal tide.

[6] SABER measurements record the geographical distribution of the state of the atmosphere at constant local solar time (SLT), which precesses slowly from day to day. This permits decomposition of tides into their various components, both migrating and nonmigrating over time periods wherein precession occurs through a complete cycle of local time. It takes 60 days for TIMED to complete a global and full diurnal picture [Zhang *et al.*, 2006], so the measurements provide information on the slowly varying mean state and are ultimately insensitive to incoherent effects such as those produced by gravity waves and planetary waves. The SABER instrument aboard TIMED makes temperature measurements that overlap with those of resonance lidars in altitude, so this provides opportunity for comparisons and coordinated studies. By focusing on the longitudinal structure of semidiurnal oscillations at 20° latitude, SABER measurements are combined with the lidar results in order to determine the spectrum of waves that contribute to the semidiurnal structures observed at Arecibo and Maui.

[7] Nocturnal lidar observations limit this study to the semidiurnal tide. The semidiurnal tide plays an important role in the balance between the low and high summer mesopause-region temperature minima and the strength of

the intervening inversion observed at midtropical and subtropical latitudes [She and von Zahn, 1998; States and Gardner, 2000a, 2000b; Chu *et al.*, 2005]. It is expected to dominate the tidal temperature perturbation at 20° latitude, as models show that the diurnal tide amplitude is near a node point, with seasonal maximum amplitudes under 5 K in the altitude range under consideration [Forbes and Garrett, 1978; Forbes *et al.*, 1997, 2006]. SABER observations concur with this prediction [Zhang *et al.*, 2006; Forbes *et al.*, 2008]. Observations made from the Upper Atmosphere Research Satellite (UARS) demonstrate that the dominance may be seasonal. Where they show semidiurnal tides to be dominant in January at 86 km and 20°N, for July they show quite small semidiurnal amplitude, a season when the diurnal amplitude is large [Forbes and Wu, 2006]. Forbes *et al.* [2008] did a similar analysis from SABER data, but for higher altitudes, which shows winter minima for both semidiurnal and diurnal thermal tides at 100 km and 20°N. However, the semidiurnal amplitude in January shows a small peak near winter solstice that has a biennial modulation. Given this knowledge, we feel that the nocturnal data sets from Arecibo and Maui, coupled with the wider diurnal longitude and latitude coverage of SABER, can reveal much about the longitudinal structure of the semidiurnal thermal tide and localized coherent effects at multiple longitudes.

[8] Although Arecibo has coverage for 12 months [Friedman and Chu, 2007], observations at Maui, undertaken during the Maui-MALT campaign [Chu *et al.*, 2005], only cover 7 months, and one of those, March, has insufficient temporal coverage to clearly reveal a 12-h oscillation. In this longitudinal comparison, we focus on 6 months covered by the Maui observations: January, April, May, July, August and October. Our goal is to make a comparison of the seasonal variability of the semidiurnal tide as observed from Arecibo and Maui and to place these results in the full longitudinal structure provided by SABER. We use SABER longitudinal and seasonal data version 1.07 from the Web site <http://sisko.colorado.edu/TIMED/SABER.html>. We also include GSWM results, extracted from the GSWM-02 (Global-Scale Wave Model–2002) Web site, <http://sisko.colorado.edu/TIMED/GSWM.html>, for comparison. From this wider longitudinal picture, lidar observations reveal locally coherent tidal structures that can result from nonmigrating or stationary perturbations.

[9] This paper is a follow-up to Chu *et al.* [2005] and Friedman and Chu [2007]. The former present initial analysis of observations from the Maui-MALT campaign with comparisons to measurements made at Starfire Optical Range (SOR), NM, and the latter describe the seasonal MLT thermal structure for Arecibo and compare it with those of Maui and SOR. These contain general information on the lidars and data processing methods that are pertinent here; thus, the reader is referred to those papers for technical details on the lidars.

2. Data Processing

[10] Lidar-measured temperatures from Arecibo and Maui are binned with resolutions of 0.5 h and 0.5 km on the same temporal and range grid and then month by month to produce composite mean nights [Chu *et al.*, 2005;

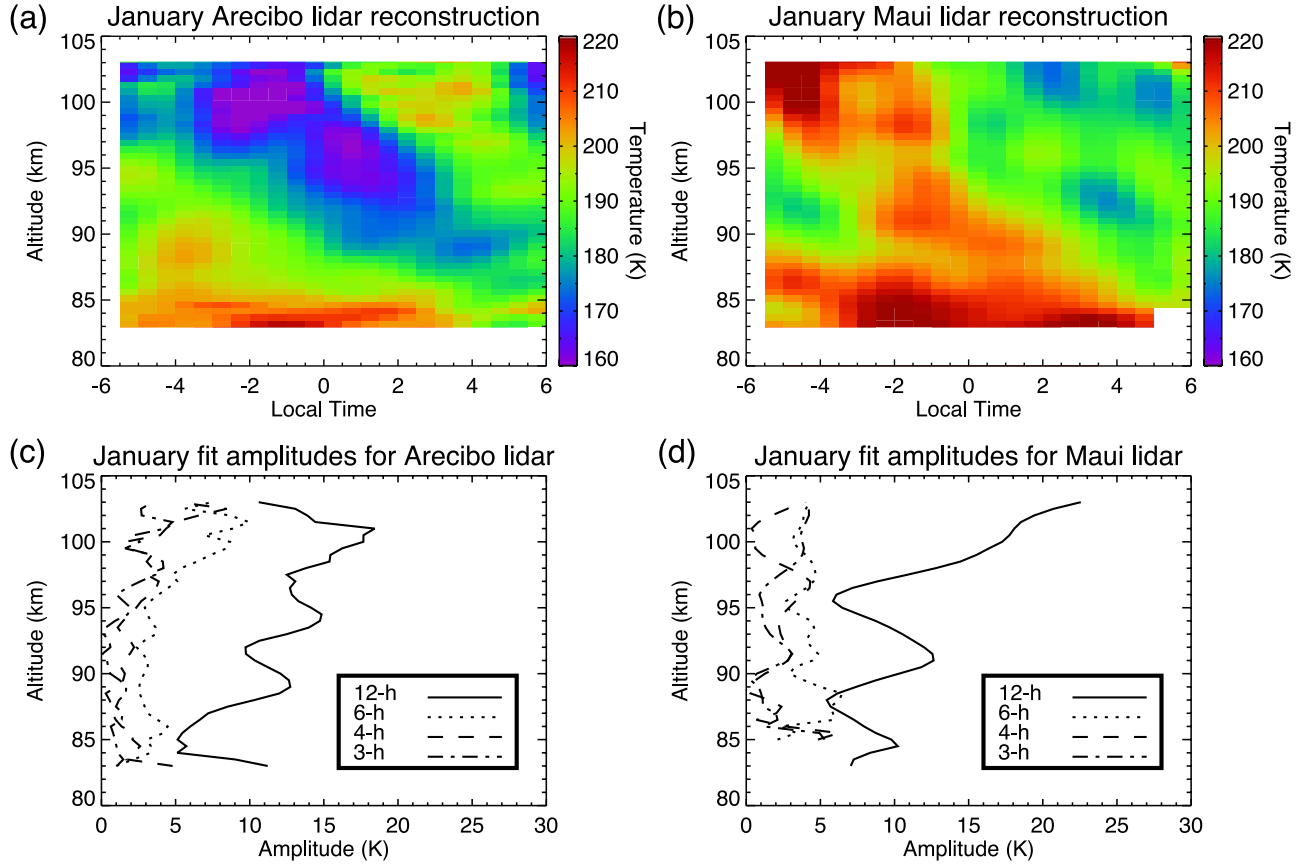


Figure 1. Reconstructed January data for (a) Arecibo and (b) Maui and (c and d) their fit amplitudes.

Friedman and Chu, 2007]. This technique results in composite mean night thermal structures with small statistical errors and incoherent wave effects averaged out. Maui lidar results are from the Maui-MALT campaign from 2002 to 2005, with different months' observations occurring in different years. SABER v1.07 data span 2002–2007. Data are then selected for the six months of observations from Maui that are amenable to this analysis: January, April, May, July, August and October. Arecibo lidar data included are from observations beginning in December 2003 and ending in April 2007, and in this paper we only consider data recorded in the months of Maui observations, though often from different years. As mentioned above, SABER data are obtained using the SABER web tool, and longitudinal thermal tide amplitudes and phases are extracted at altitudes of 86, 90, 94, 98, and 102 km for the months under consideration.

[11] We fit the lidar data at each altitude bin to a 12-h modulation using equation (1):

$$T(z, t) = T_0(z) + A_1(z) \cos\left(\frac{2\pi}{12}t\right) + A_2(z) \sin\left(\frac{2\pi}{12}t\right), \quad (1)$$

resulting in the following parameters:

$$\Delta T_{12}(z) = \sqrt{A_1^2(z) + A_2^2(z)} \quad (2a)$$

$$\phi_{12}(z) = \left(\frac{12}{2\pi}\right) \tan^{-1}(A_2/A_1), \quad (2b)$$

where $T(z, t)$ is the temperature at a given altitude and time, $T_0(z)$ is the mean temperature at altitude z , ΔT_{12} is the oscillation amplitude, and $\phi(z)$ is the phase in local time. We attempted the fit using both uniform weighting and weighting by the number of observations at a given range-time and kept the result with the best goodness-of-fit parameter. Generally, the best fit resulted from uniform weighting or there was marginal difference. The residuals are fitted to 6-h, 4-h and 3-h oscillations in order to confirm that the 12-h modulation is dominant. An example of the results, for January, are plotted in Figure 1, where we have reconstructed the thermal profiles on the basis of the fits, so any higher-frequency components are removed. The 12-h modulation stands out above other frequencies throughout the altitude range for both sites, and we focus on that oscillation here.

[12] In the following, the semidiurnal amplitudes and phases for Arecibo and Maui lidars are compared. These are considered in light of the 12-h amplitudes and phases measured by SABER. The identification of various semidiurnal oscillations identified in the SABER results are compared with the integrated lidar-observed results. The methodology for extracting semidiurnal tides from the TIMED/SABER data is fully described by Forbes et al. [2008].

3. Sampling Effects: Compensating for the Diurnal Tide

[13] The lidars make spot measurements at precise locations with continuous temporal coverage during any given

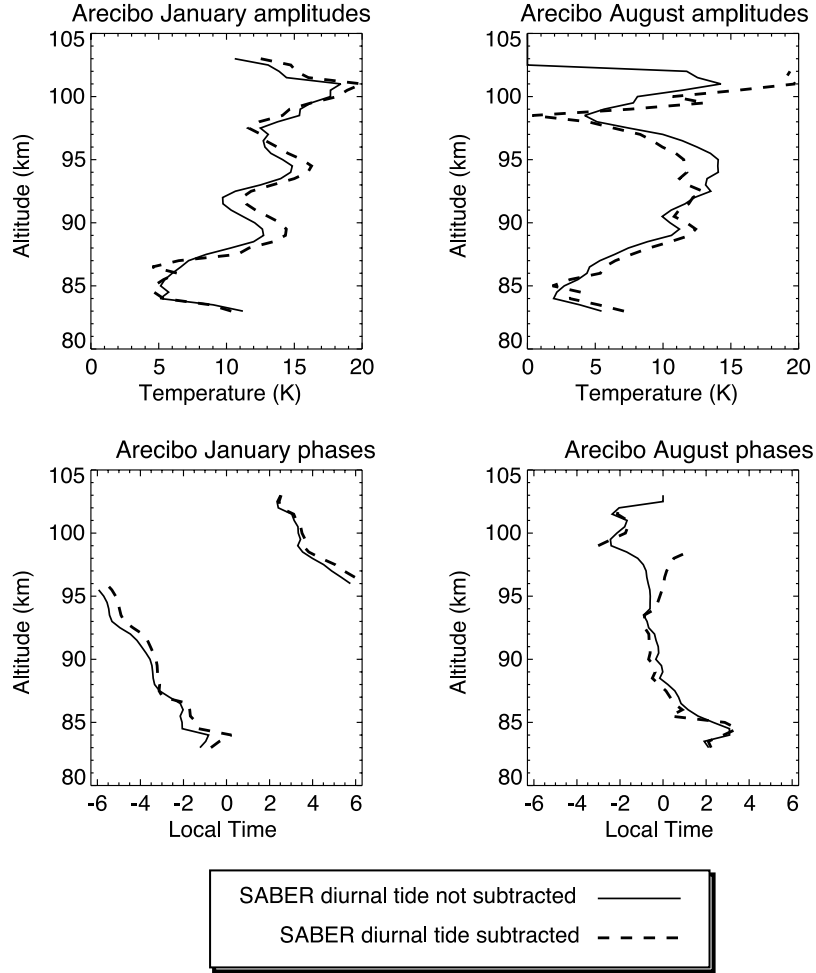


Figure 2. Plots of semidiurnal (top) amplitudes and (bottom) phases for (left) January and (right) August for Arecibo. The solid lines are computed directly from the data set, while the dashed lines have had the diurnal component, as measured by SABER, removed.

night. The monthly averages used here remove only temporally incoherent effects. They will be sensitive to locally coherent effects, even if those effects do not have geographic extent. SABER, on the other hand, cannot make such precise spot measurements, and it requires 60 days to provide a full temporal picture. The geographic window for SABER for a given location is about $\pm 5^\circ$ (or ± 600 km) latitude and longitude. This temporal and geographic averaging means that SABER is not sensitive to short-term temporal or limited geographical coherent oscillations.

[14] The lidar measurements presented here are nocturnal only. This fact leads to the question of whether the diurnal tide may contaminate the semidiurnal tides computed from these data. To this end, we have evaluated two months, January and August, using SABER-measured diurnal tide amplitudes and phases for both locations to remove diurnal tide-induced bias. The two months, January and August, present extremes in the results, with minimal agreement between the two sites, or between the lidars and SABER, in January, and much better correlation in August, as discussed further in section 5.

[15] In Figure 2, we show the results for Arecibo. In neither January nor August is there a substantial difference, whether or not the SABER-measured diurnal tide is removed.

The subtle differences are not much larger than the typical uncertainties in the fitting, which are ~ 0.5 K for the amplitudes and < 0.5 h for the phases. In Figure 3, for Maui, we see that there is a notable increase in the semidiurnal amplitudes when the diurnal tide is removed, except for January above 97 km where the semidiurnal amplitude decreases when the diurnal tide is removed, indicating that in most cases the aliasing artificially reduces the semidiurnal amplitude.

[16] For the purposes of this report, we do not remove the SABER diurnal tides from the lidar. This is because in the cases where there is disagreement between the SABER and lidar results, the addition of the diurnal modulation does not make the two measurements more similar. Also, if the semidiurnal tides can be so different at a specific location than that of the broader regional and temporal average, this may also be the case for the diurnal tide, so using SABER results to provide a diurnal tide representation for the individual lidar results has questionable validity.

4. Results

[17] In this section, we compare the semidiurnal amplitudes and phases measured by the lidars at Arecibo and Maui with those recorded by SABER for the two locations

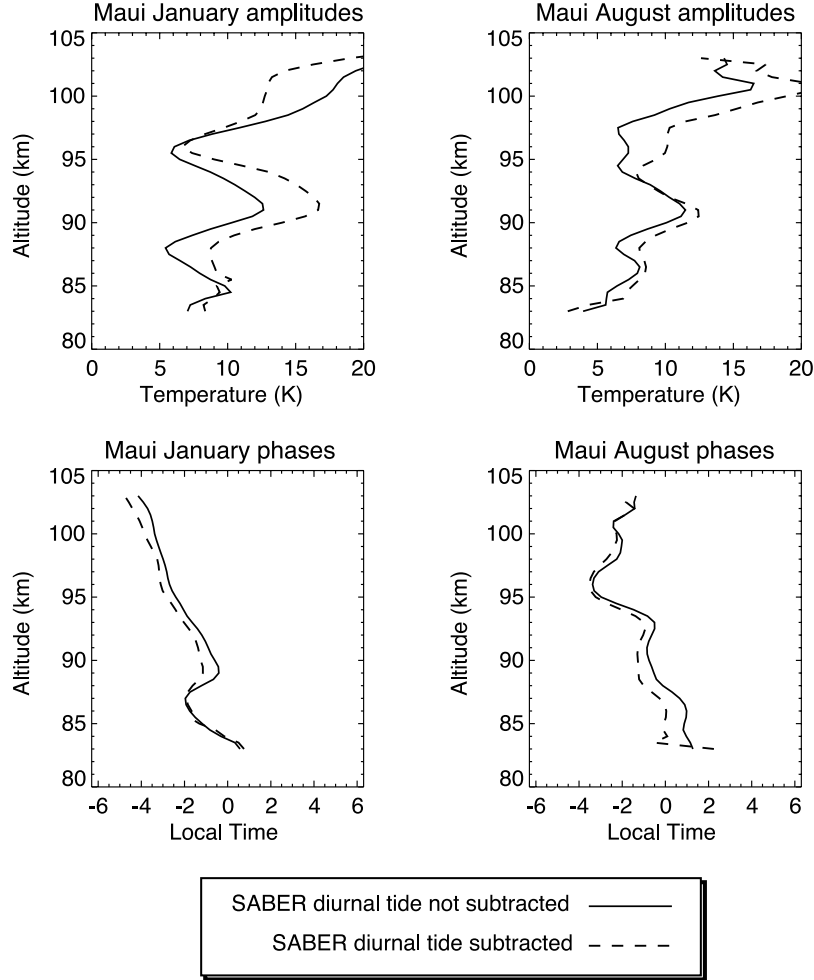


Figure 3. Plots of semidiurnal (top) amplitudes and (bottom) phases for (left) January and (right) August for Maui. The solid lines are computed directly from the data set, while the dashed lines have had the diurnal component, as measured by SABER, removed.

and show how these fit into the longitudinal picture given by SABER measurements. For the local measurements, we include results from the GSWM-02 model for comparison as well. In what follows, we look at similarities and differences between the two locations and between each of them and the corresponding measurement by SABER. Similarities indicate the primary influence of the migrating tide. Explanation of differences is far more complex and must include results from nonmigrating effects that maintain their coherence so as to be revealed in these monthly and interannual averages.

4.1. Semidiurnal Results for Maui and Arecibo

4.1.1. Semidiurnal Amplitudes

[18] Figure 4 shows the semidiurnal amplitudes for the 6 months of lidar results from Arecibo (red solid lines) and Maui (blue dashed lines), coupled with SABER measurements for both sites (red diamonds denote Arecibo; blue triangles denote Maui). Also included are results of the GSWM-02 model for Arecibo (red pluses) and Maui (blue asterisks) [Hagan and Forbes, 2002, 2003]. The GSWM amplitudes are quite similar for each month at both sites, indicating dominance of the migrating tide in the model. In

contrast with the GSWM-02 calculations, the observed amplitudes for Arecibo and Maui, both from the lidars and SABER, show differences at some altitudes and similarities at others, indicating that there are local effects that modulate the tide in consistent, though longitudinally varying, ways. Lidar observations from the two sites do show rough agreement in the tidal amplitudes. This, given that the observations were not undertaken simultaneously or even on the same years, argues against large and consistent localized 12-h forcings at the two sites. It is also not surprising that there are considerable differences between the SABER and lidar amplitude measurements. The lidars make spot measurements with exact monthly binning in contrast to SABER's necessarily broader geographical and temporal averaging. The lidars also record data more sparsely, as their operations are determined by user, facility and weather conditions. Thus, the fact that both lidar sites see considerably larger amplitudes in the winter month, January (particularly Maui, where SABER sees a very weak semidiurnal tide), can be attributable to the different sampling, which makes the lidars more sensitive to locally enhanced (or diminished) tides. Factors that cause local amplification (or deamplification) may include consistent

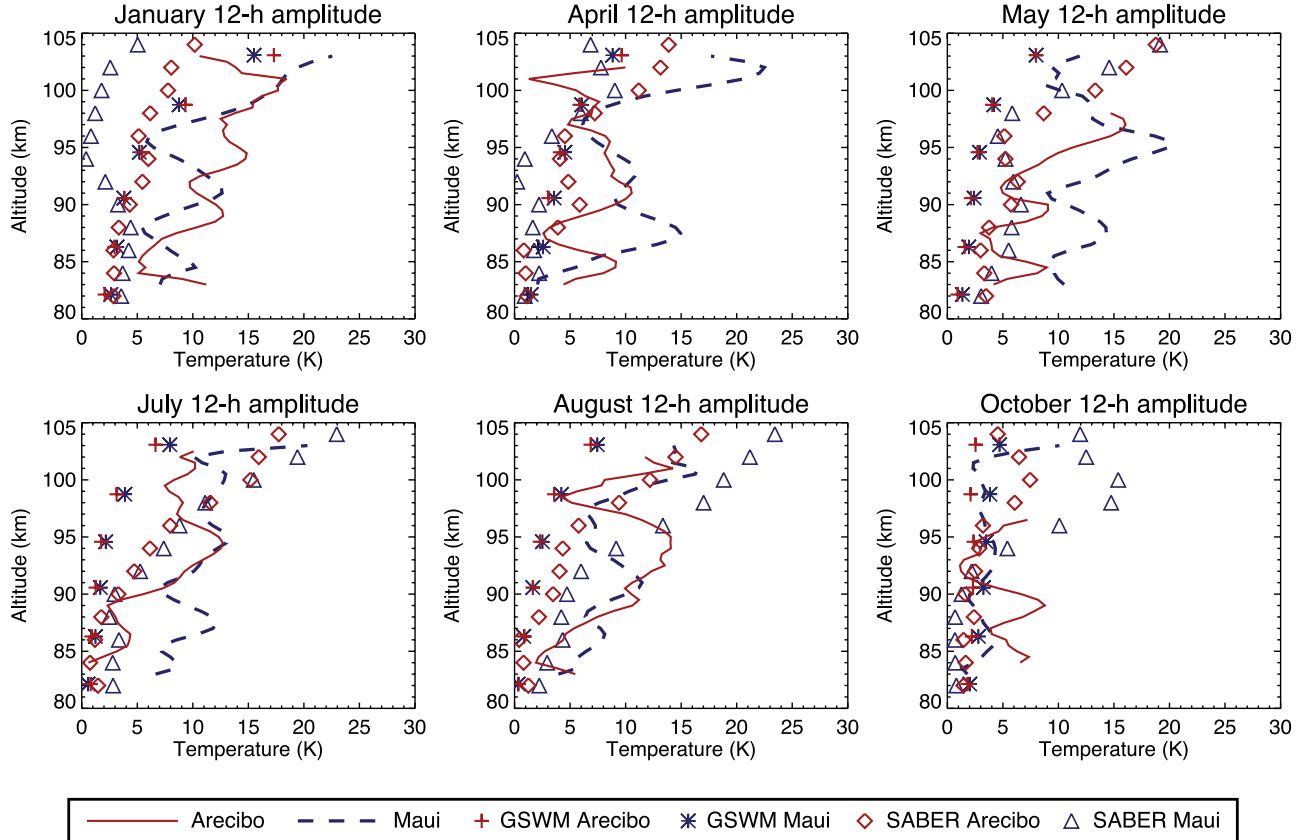


Figure 4. Semidiurnal temperature tide amplitudes as measured by the Maui (blue dashed lines) and Arecibo (red solid lines) lidars for January, April, May, July, August, and October. SABER amplitudes are given for Maui (blue triangles) and Arecibo (red diamonds). GSWM-02 results are also shown for Maui (blue asterisks) and Arecibo (red pluses).

gravity wave activity that coherently modulates the tide, enhancing or diminishing its amplitude [see *Forbes et al.*, 1991, and references therein]. While for other months the lidar-SABER comparison is better than that for January, it is interesting to note that for Maui in August and October, SABER observes larger amplitudes above 95 km than the local lidar measurements. The seasonal variation presents questions as well. The lidar sites see semiannual variation, with maxima during solstices, while SABER sees an annual variation with maximum amplitudes in summer, and GSWM-02 also produces an annual variation but with the maximum in winter. At the lower altitudes, SABER does have better agreement with the lidar, with larger amplitudes in solstices than in equinoxes.

4.1.2. Semidiurnal Phases

[19] Figure 5 shows the corresponding semidiurnal phases for these months for Arecibo and Maui measured by lidar and SABER along with the GSWM-02 results for comparison. They are plotted with respect to SLT, so, as with the amplitudes (above and Figure 4), a migrating tide will generally produce the same structure for both locations. The lidar-measured phases are in quite close agreement with one another for all months but January. In that month the Arecibo phase shifts by $\sim 90^\circ$ from while for Maui the phase shifts by $\sim 45^\circ$. This shift indicates the presence of a dominant nonmigrating tide that has driven one or both of the sites' modulations away from the principal migrating

tide. It is interesting that the SABER January measurements agree quite well with the Maui lidar below 93 km, but diverge above, while the inverse is true in the comparison over Arecibo, where there is agreement above 95 km but not below. This will be further discussed in section 5.

[20] One feature of the phase structure for several months that is reflected in the SABER and GSWM-02 results is the steep phase front, indicating a long wavelength, at lower altitudes. This is often (e.g., April, May and August) evanescent, or nearly so, below 90–92 km. This structure is not seen so consistently in the lidar results, but it is visible in May for both sites, and in July and August for Maui. There is not consistent agreement between the measured phases and those predicted by GSWM-02. However, agreement is better for equinox seasons than solstices. One exception is that GSWM-02 matches the measured phase for Arecibo in January above 95 km. More commonly, GSWM-02 computed phases for solstice months are 90° off from those measured.

4.2. Longitudinal Structure

[21] Figures 6–11 show the mean longitudinal morphologies of the semidiurnal tide amplitude and phase as measured by SABER from 2002 to 2007. Figures 6–11 (left) show tidal phase as a function of longitude at altitudes (from bottom to top) of 86, 90, 94, 98 and 102 km, and Figures 6–11 (right) show similar plots for amplitudes at

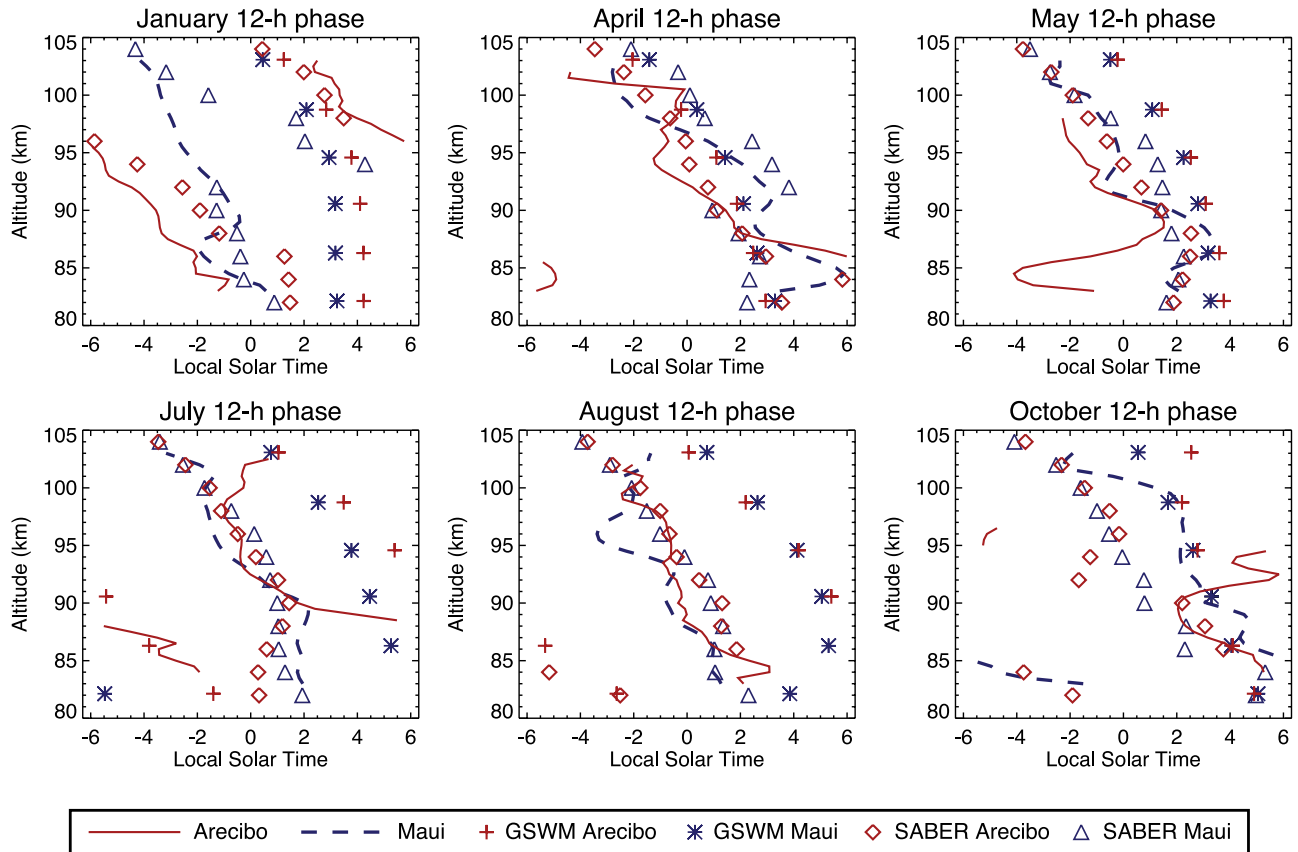


Figure 5. Semidiurnal temperature tide phases as measured by the Maui (dashed blue lines) and Arecibo (solid red lines) lidars for January, April, May, July, August, and October. SABER amplitudes are given for Maui (blue triangles) and Arecibo (red diamonds). GSWM-02 results are also shown for Maui (blue asterisks) and Arecibo (red pluses).

each altitude. The solid square in each plot represents the value for Maui at the altitude of the plot, and the solid triangle shows that for Arecibo. Below, these plots will be referred to as “longitude plots.”

4.2.1. January

[22] Figure 6 shows the longitude plots for the month of January. There are two prominent features in the January SABER results. One of these is the appearance of rapid phase modulations, one of which occurs at 94 km coincident with Maui’s location. The other is a strong wave-2 amplitude structure at the higher altitudes. As for comparisons with the lidar, there is apparent good agreement in the phase measurements, although Figure 5 shows this is deceptive, particularly for Maui, as the SABER-measured phase for Maui shifts 15 h between 93 and 102 km, while over the same range the lidar-measured phase shifts only 3. SABER-measured semidiurnal amplitudes are less than their lidar-measured counterparts throughout the altitude range. This is particularly pronounced for Maui, where SABER shows a node in the wave-2 zonal semidiurnal amplitude structure (mentioned above) at 204°E, but the lidar-measured amplitudes are quite comparable with those measured at Arecibo. Unlike for Maui, at Arecibo’s longitude, 293°E, SABER measures quite appreciable amplitudes throughout the altitude range coincident with the lidar. However, these are still only about half of what the lidar

measures at most heights. These differences could be related to local effects observable by the lidar, but which are smoothed over by the necessarily large geographic sample that SABER observes. Temporal effects can contribute as well, as SABER tides require 60-day averages, rather than the monthly binning by the lidar. The differences between SABER and lidar-measured semidiurnal tide for Maui in January are definitely intriguing and merit further study.

4.2.2. April

[23] In Figure 7 we plot the longitudinal comparison between SABER, Maui and Arecibo for April. As already shown in Figure 5, the phase agreement is quite good for both sites, while for Maui the amplitude measured by the lidar is much larger throughout the altitude range than that for SABER. The acute longitudinal phase variation observed in January is not apparent for April, except at the 86 km altitude near Arecibo’s longitude. Nevertheless, the phase agreement is quite good between SABER and Arecibo. In the SABER amplitudes, there is a wave-4 pattern, and the longitude of Maui falls in a minimum amplitude region throughout the 86–102 km altitude range displayed. In fact, this is also the case for Arecibo. In spite of this and the generally reduced semidiurnal amplitudes observed in April, the lidar-measured amplitudes are generally larger than those observed by SABER. Near the altitude range 92–95 km, where SABER sees amplitude minima for both

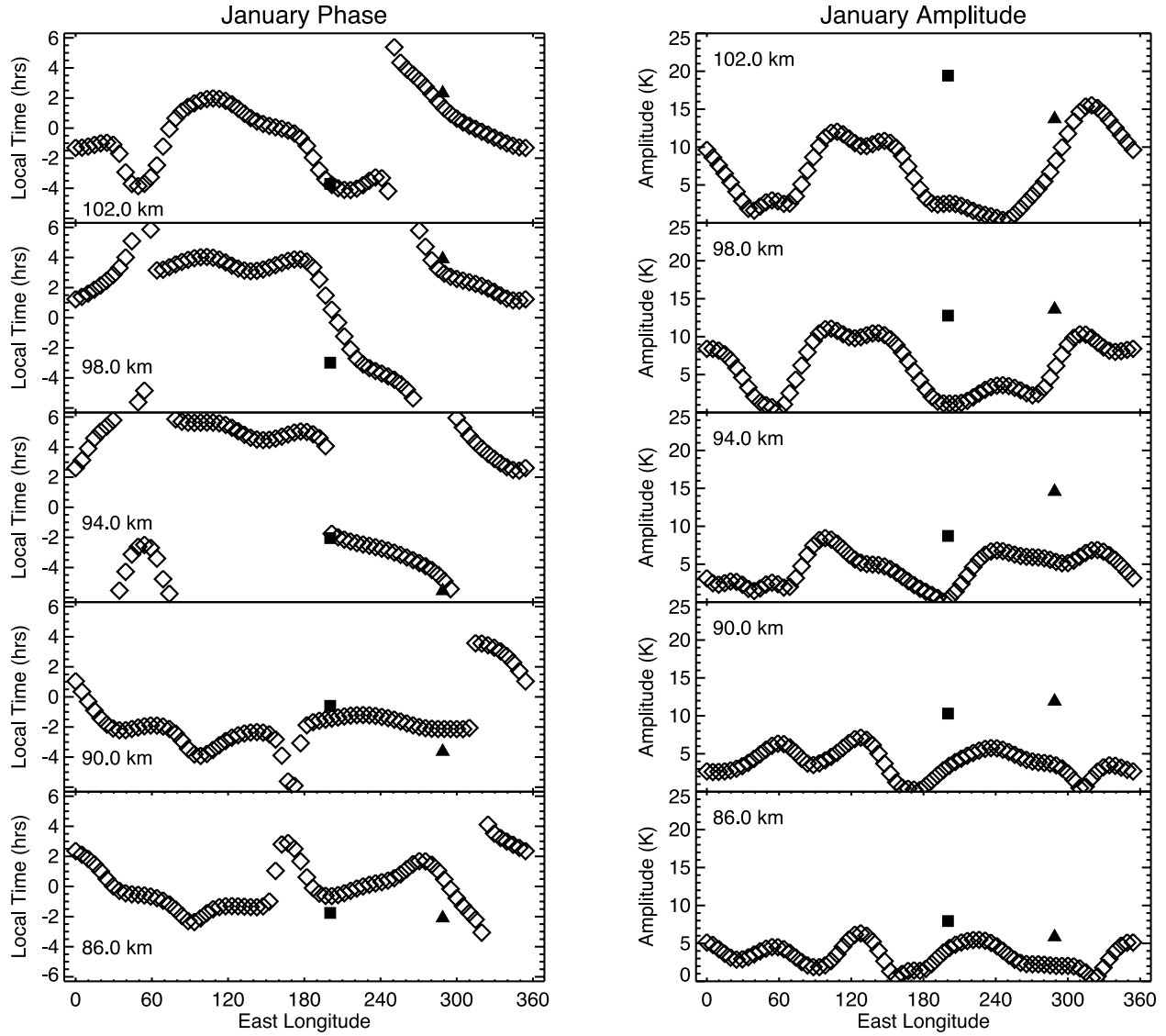


Figure 6. January measurements of (left) phase and (right) amplitude of the semidiurnal tide versus longitude made by SABER (open squares) and lidars at Maui (solid squares) and Arecibo (solid triangles). From bottom to top are results from 86, 90, 94, 98, and 102 km altitude.

locations, the lidars see relative maxima as shown in Figure 4.

4.2.3. May

[24] Figure 8 shows that in May, as in April, the phase structure for both lidars are good agreement with SABER measurements for their locations. The longitudinal phase structure is smooth and has little variation compared to January or April. The longitudinal semidiurnal amplitude structure has a wave-5 structure in the mesopause region. Neither Maui nor Arecibo falls in amplitude nulls of that structure, and there appears to be better agreement between the lidar and SABER amplitudes, particularly for Arecibo. In the case of Maui, as for January and April, SABER amplitudes are smaller than those measured by the lidar, except in this case at the highest altitudes, 100 km and above, where the SABER amplitudes exceed those measured by the lidar. Between 98 and 102 km, the amplitude measured by SABER increases by a factor of 3 while that

for Maui lidar falls. Arecibo lidar measurements do not give reliable semidiurnal results for altitudes above 98 km.

4.2.4. July

[25] In July (Figure 9) there is quite reasonable all-around agreement between the SABER and lidar amplitude and phase profiles as shown in Figures 4 and 5. The longitudinal phase structure has some rapid variation in the 90 and 86 km plots west of Maui. The amplitude structure has a predominantly wave-4 structure, and both sites fall near maximum amplitudes at higher altitudes. The fact that the lidars see maxima in semidiurnal tidal amplitudes for both solstices, while for SABER it is only for midsummer may be related to the phase of the wave-4 structure as well as to local modulations and sampling effects.

4.2.5. August

[26] For August, the results are quite similar to those for July. However, the SABER-measured longitudinal amplitude structure is wave-5 in this case. The phase structure is

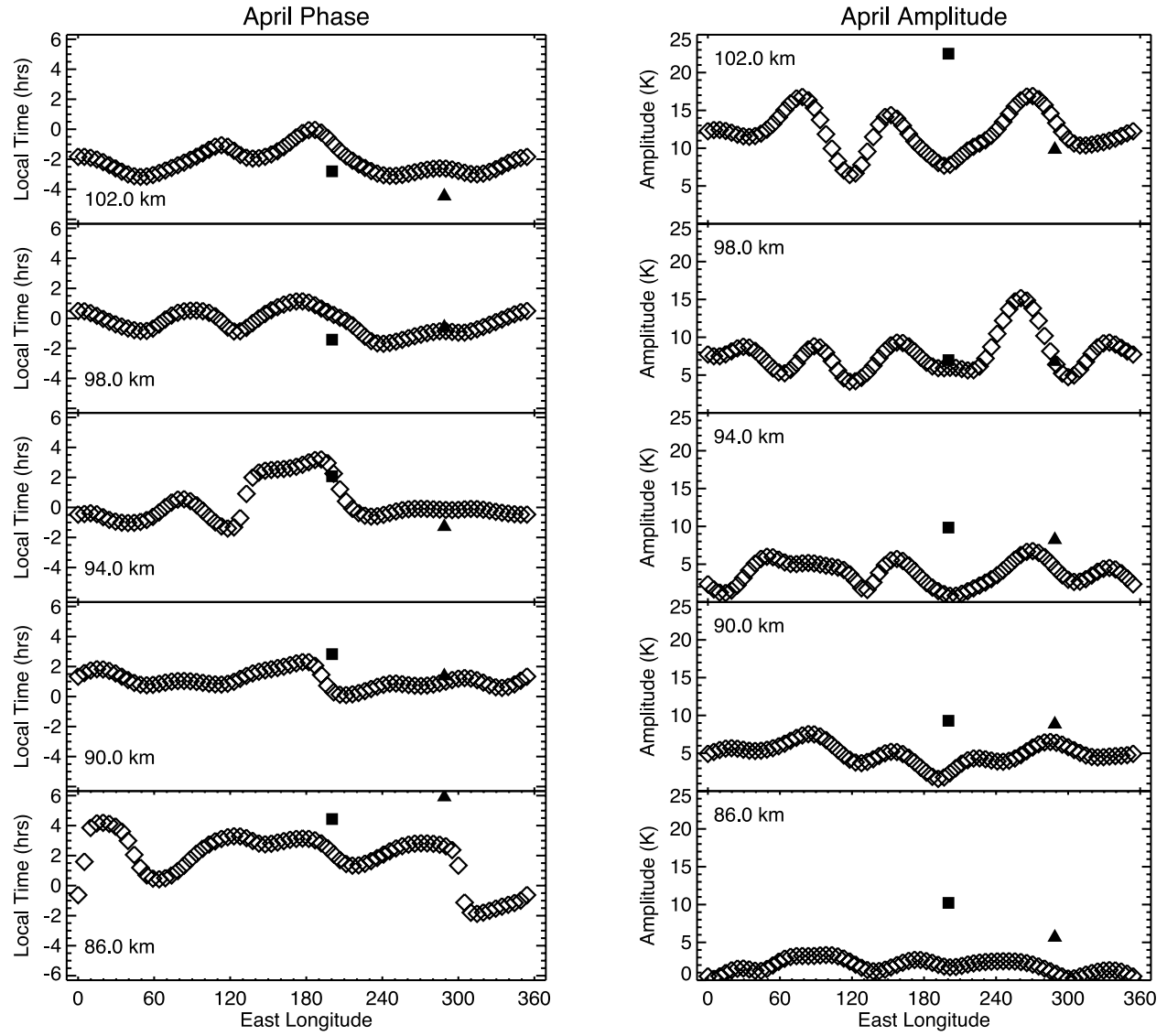


Figure 7. April measurements of phase (left) and amplitude (right) of the semidiurnal tide versus longitude made by SABER (open squares) and lidars at Maui (solid squares) and Arecibo (solid triangles). From bottom to top are results from 86, 90, 94, 98 and 102 km altitude.

unremarkable except for a 2.5-h phase jump at 86 km near Arecibo's longitude. From Figures 4 and 5 we see good agreement between SABER and lidar measurements, and these are reflected in Figure 10. The SABER amplitudes exceed those measured by lidar somewhere in the mid-90-km range, which was not observed for earlier months. Maui's longitude is near a maximum in the wave-5 structure, while Arecibo is close to a minimum.

4.2.6. October

[27] The longitudinal structures for October are shown in Figure 11. There are no sharp transitions in phase as seen in some other months, but there is more variability than other months at the lower altitudes. Other than at the very lowest altitudes, SABER measures a phase \sim 2-h earlier than observed by the Maui lidar. The case of Arecibo is less clear, as the lidar altitude does not extend very high, but there is good agreement at 86 and 90 km, while the SABER phase leads by 6 h at 94 km. For October, the lidar-

measured amplitudes are quite small, as shown in Figure 4. The fact that Maui again falls near a longitudinal wave-4 amplitude minimum is reflected in the small amplitude, yet the lidar-measured small amplitude extends throughout its measurement range, except above 102 km, while SABER sees increasing amplitude above 95 km, reaching 15 K at 100 km where the lidar measures only 3 K.

5. Discussion

[28] A feature of the semidiurnal thermal tide structure in the tropical MLT region is the seasonal nature of the phase front. In this comparison, we see that Arecibo and Maui have similar phase structures throughout the year, except for January. Looking at the zonal phase structure for these months, we see that during most seasons the phase variation with longitude is fairly small for all months except January. SABER results show that the phase structure in January

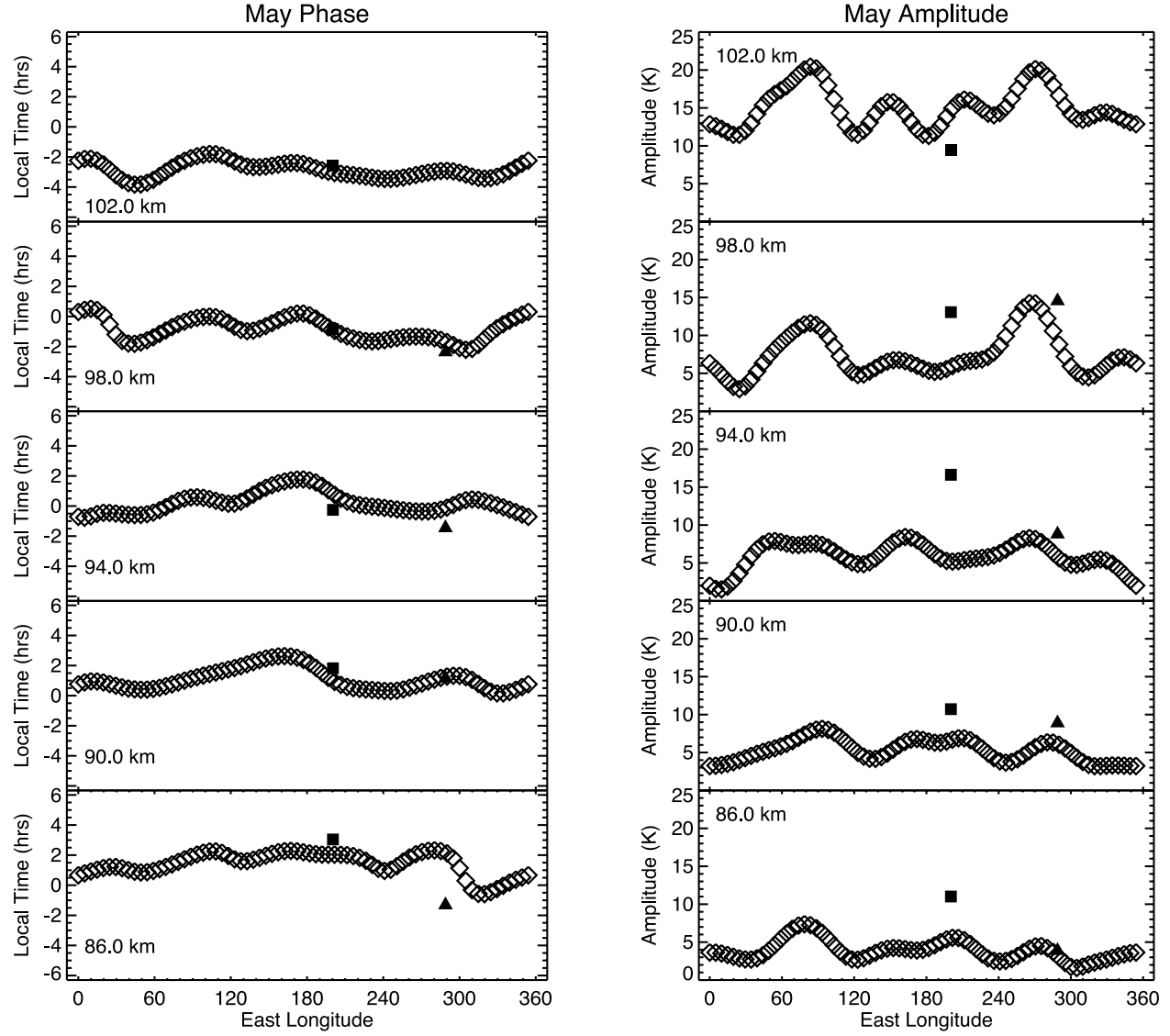


Figure 8. May measurements of (left) phase and (right) amplitude of the semidiurnal tide versus longitude made by SABER (open squares) and lidars at Maui (solid squares) and Arecibo (solid triangles). From bottom to top are results from 86, 90, 94, 98, and 102 km altitude.

varies through a complete 12-h cycle, and Arecibo and Maui fall in different locations on that cycle. This indicates that nonmigrating oscillations have a strong influence for that season. At higher altitudes (>90 km), the phase in January is 6 h (90°) off of that measured for the other months. This shift may be indicative of asymmetric forcing of the tide. Given the relatively short wavelength typically seen at these altitudes (25–45 km), this seems indicative of a fairly high-order dominant mode, such as $(s, n) = (2, 5)$, where s is the longitudinal wave number (2 for semidiurnal) and n is the “order” parameter and is related to the altitude and latitude structure [Chapman and Lindzen, 1970; Forbes, 1995]. At lower altitudes, however, the seasonal difference is not so pronounced. Below 85 km, the lidars see the phase between 2200 and 0200 SLT in January, while for other months it is not consistent, though it generally falls after midnight. Higher-order (shorter wavelength) modes are not expected to penetrate into the thermosphere [Forbes and

Garrett, 1979], so it is conceivable we are seeing a transition between a region where higher-order modes dominate to one where lower orders dominate. The Arecibo measurement at its highest altitudes is in good agreement with the semidiurnal temperature phase measured by incoherent scatter radar [Salah et al., 1991; Zhou et al., 1997]. In a January 1993 10-day World Day experiment the semidiurnal temperature tide was measured from ~ 100 to over 140 km. A wavelength of over 50 km was observed [Zhou et al., 1997, Figure 8a], which is not in good agreement with the Arecibo lidar observations below 105 km, although there is reasonable agreement in the phase times at 100 km altitude.

[29] Another feature of the phase structure that is commonly observed in the SABER profiles, though less prominent in the lidar, is that the phase front is steep at lower altitudes and shallow at higher altitudes. SABER sees this phenomenon in all months but October, and it is common to

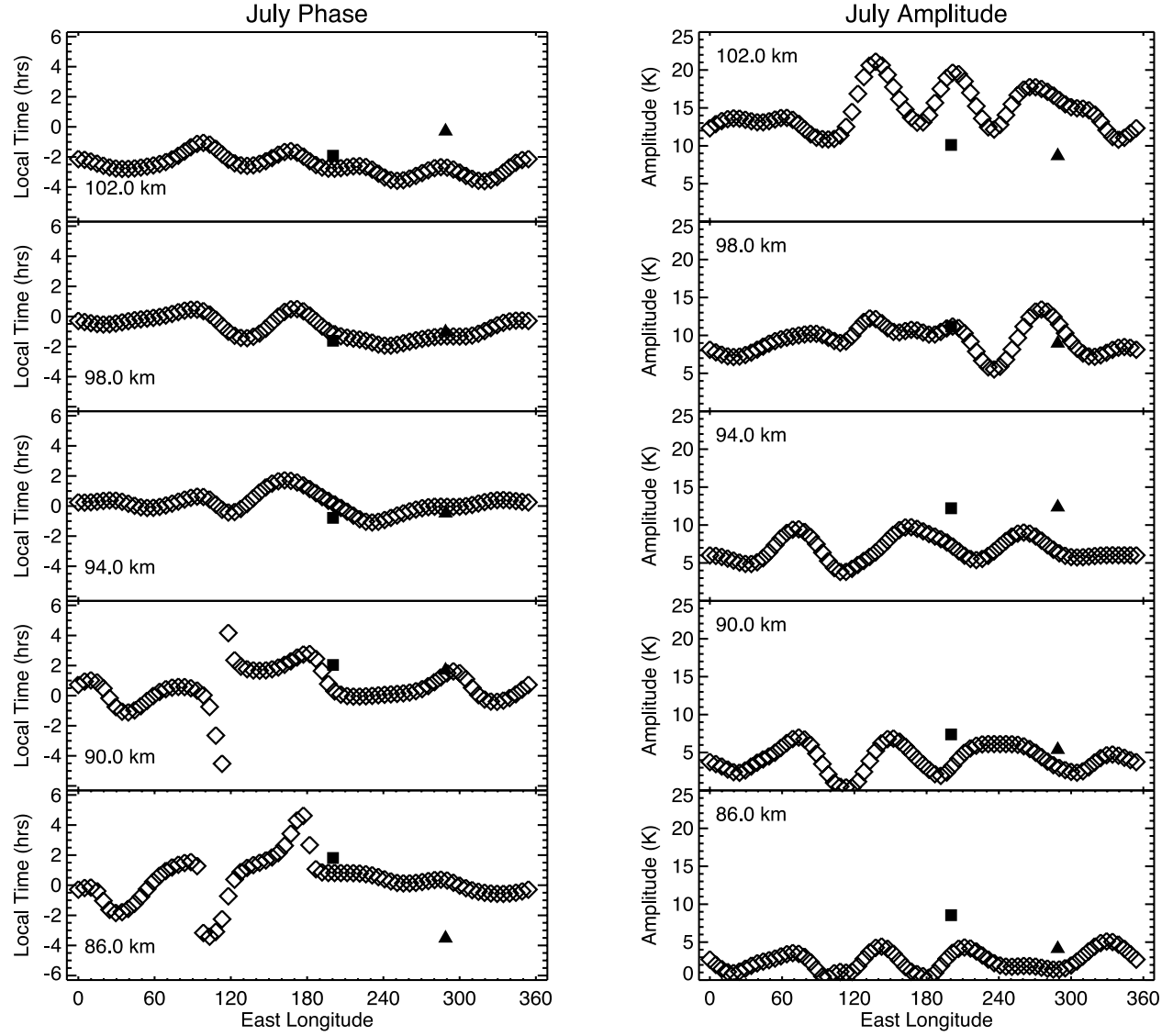


Figure 9. July measurements of (left) phase and (right) amplitude of the semidiurnal tide versus longitude made by SABER (open squares) and lidars at Maui (solid squares) and Arecibo (solid triangles). From bottom to top are results from 86, 90, 94, 98, and 102 km altitude.

GSMW-02 profiles as well. The lidar results are less clear, although there is some hint of this structure in May, July, August and October. The steep phase front, indicating a very long wavelength, is indicative of the main (2, 2) tidal mode [Chapman and Lindzen, 1970; Forbes, 1995]. That the phase front gets shallower (shorter wavelength) at higher altitudes, may indicate that the (2, 2) mode does not penetrate through the mesopause, while higher-order modes either do penetrate or are generated at mesopause heights. However, as we discuss below, SABER modal decomposition produces a shallow (2, 2) mode as high as 110 km. The lidars occasionally see evidence of the contrary condition, where the longer wavelength mode is observed at higher altitudes, and the wavelength is shorter at lower altitudes. This can be seen for Arecibo in April and July, and for Maui in August. Unfortunately, the observations do not extend to high enough altitudes to provide a definitive result.

[30] The lidar-measured semidiurnal amplitude is larger during solstice periods than equinox periods for both

Arecibo and Maui, indicating a semiannual variation. The SABER measurements are not in good agreement with this seasonal structure. In particular, SABER does not see the large winter amplitudes recorded at both sites, while it does see increased amplitudes following the summer solstice (May amplitudes are small while July and August amplitudes are large), as compared to the equinox months. This indicates an annual variation with a maximum in late summer. As seen in Figure 5, the GSMW-02 model indicates a maximum in semidiurnal amplitude in winter, with smaller amplitude during the remainder of the year, particularly in October, when the amplitude is small throughout the lidar measurement range.

[31] Motivated by the shallow semidiurnal phase front consistently observed at higher altitudes, we carried out a modal decomposition of the semidiurnal tides as observed by SABER. Figure 12 shows the amplitudes between 40 and 120 km of the $s = 2$ modes for each of the 6 months considered. The (2, 2) mode is prominent for 5 of the

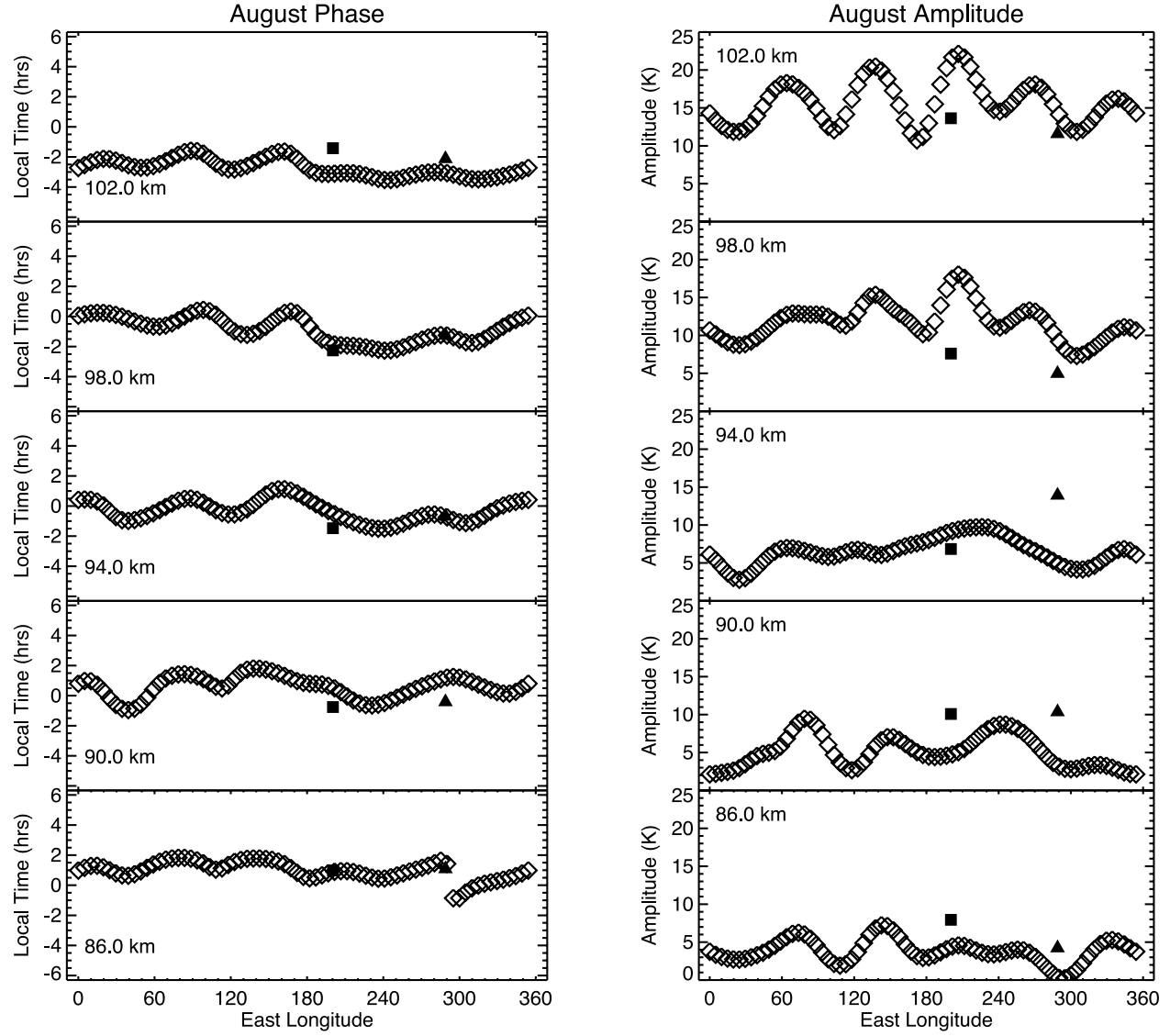


Figure 10. August measurements of (left) phase and (right) amplitude of the semidiurnal tide versus longitude made by SABER (open squares) and lidars at Maui (solid squares) and Arecibo (solid triangles). From bottom to top are results from 86, 90, 94, 98, and 102 km altitude.

6 months, excepting October. In January and July it is the predominant mode. The (2, 3) mode is inconsequential in January. However, above 90 km it begins to grow in April, is important in May and July, is predominant in August along with (2, 2), and begins to fall again in October. The (2, 4) mode amplitude is fairly constant throughout the year, but it has its greatest impact in equinox months and is a minor player otherwise owing to the relative strengths of (2, 2) and (2, 3). Finally, the impact of the (2, 5) mode is comparatively quite small. Tidal theory would have us expect that short semidiurnal wavelength implies dominance of higher-order modes, but the amplitudes of (2, 4) and (2, 5) belie this expectation. In Figure 13, we plot the phase structure for the $s = 2$ modes. What is remarkable here, and mentioned above, is that the propagating (2, 2) mode generally has a much shallower phase slope in the MLT than anticipated from theory. This means that the semidiurnal tides observed by the lidars, which tend to have

short wavelengths, may still be primarily the principal migrating (2, 2) mode.

[32] The results here show that the tidal phases observed by lidars at Arecibo and Maui generally concur with those measured by SABER. The notable exceptions would be for Maui in January and both sites in October above 90 km. January is notable for its particularly shallow phase front throughout the 80–105 km altitude range. The Maui lidar records a steeper phase front (wavelength ~ 30 km) than SABER (wavelength ~ 15 km above 95 km). The observed differences in semidiurnal phase structure as measured by lidar and SABER must be the result of local effects, which may also produce the much larger lidar-observed amplitudes. In October, the SABER and lidar-recorded phase slopes are very similar, but the SABER measured phase leads that of the lidar by ~ 2 h. Here it appears that local effects reduce the tidal amplitudes. It is interesting that this is seen in the autumn month but not in spring (April–May).

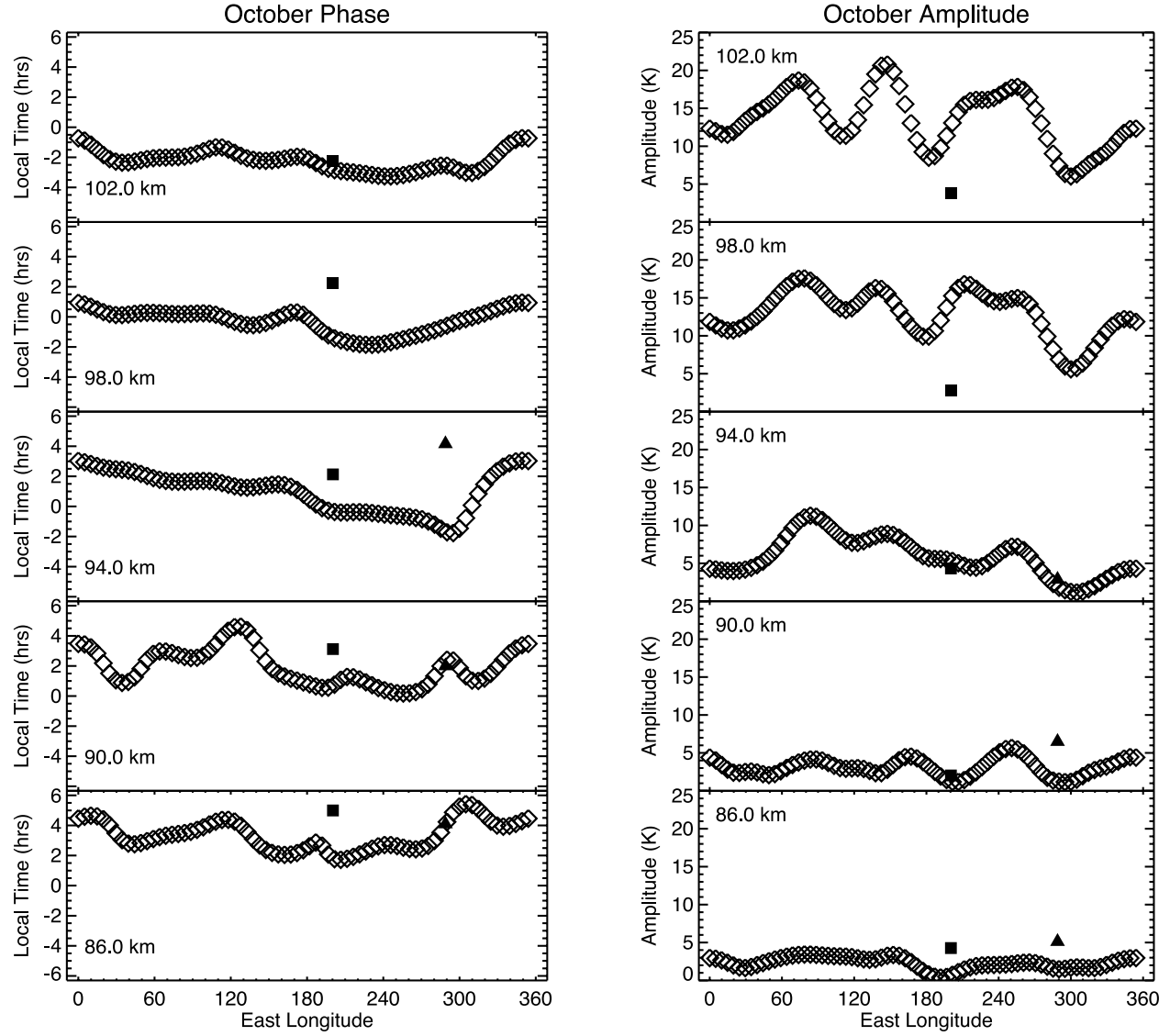


Figure 11. October measurements of (left) phase and (right) amplitude of the semidiurnal tide versus longitude made by SABER (open squares) and lidars at Maui (solid squares) and Arecibo (solid triangles). From bottom to top are results from 86, 90, 94, 98, and 102 km altitude.

For July and August the amplitudes and phases are in remarkably good agreement, indicating that the propagating tide dominates.

[33] It has previously been established [Zhang *et al.*, 2006], and is apparent in Figures 6–11, that there is a wave-4 structure in the longitudinal variation of the semidiurnal tide. This structure is the result of the distribution of continental masses with longitude and their localized impact on heating in contrast to that over bodies of water. This longitudinal modulation of atmospheric heating produces planetary waves, as well as nonmigrating tides. On a finer scale, local convective effects can also be important. In tropical regions, convection is almost a daily occurrence for much of the year, and wind flow over orography is ubiquitous, particularly for Hawaii with its tall mountains. These may make locally coherent oscillations that influence the lidar-observed tidal structure. In order to account for all of these factors, and their impacts relative to that of the

migrating tide, observations from many longitudinally distributed sites at the same latitude are required. These effects are also seasonal, and a careful study of waves and their propagations in these regions will be required to paint a clearer picture of what we have observed.

6. Summary and Conclusions

[34] In this paper, we have presented a study of the longitudinal structure in the thermal semidiurnal tide in the tropical mesopause region using measurements by the SABER instrument aboard the TIMED satellite and lidar observations from the Arecibo Observatory, Puerto Rico, and Maui, Hawaii. This study covers the months of January, April, May, July, August and October. The seasonal patterns that we have tried to capture correspond to a steady state oscillation with fixed frequency, and as such are comparable to semidiurnal tides simulated in models such as the

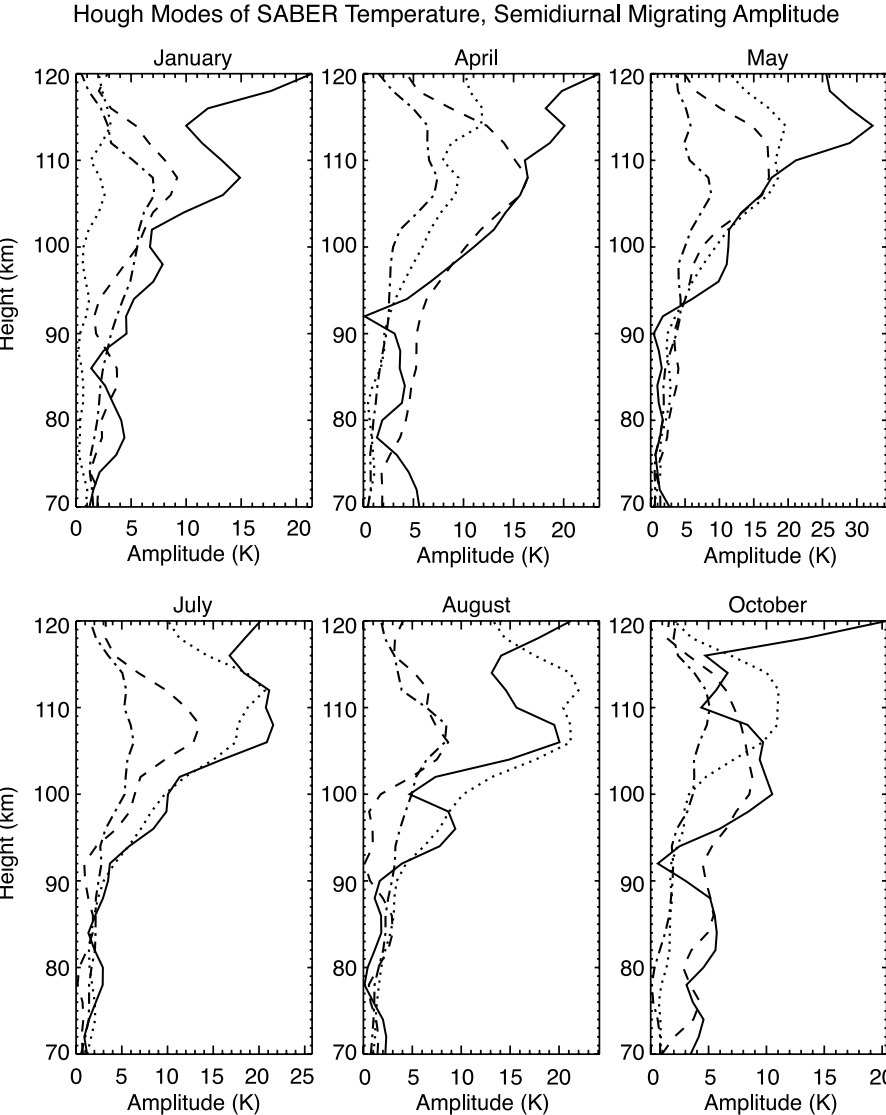


Figure 12. Amplitudes of the semidiurnal Hough modes from SABER observations for the 6 months covered in this report. Plotted are (2, 2) (solid line), (2, 3) (dotted line), (2, 4) (dashed line), and (2, 5) (dash-dotted line).

GSMW. Departures from this mean climatological state are due to transients associated with variations in wave sources, propagation conditions, and wave-wave interactions. The different ways in which the ground-based and space-based methods sample the total (mean + transient) fields of course leads to differences in the derived mean climatological states. A major goal here has been to better understand the extent of these differences. Here, we summarize the results and suggest future measurements.

[35] The lidar-observed amplitudes are generally larger than those observed by SABER, and we attribute that first to sampling effects and second to local amplification by non-migrating sources. In August and October, SABER observes larger amplitudes than the lidar at high altitudes (>95 km). This is likely due to localized reduction of tidal amplitudes that SABER observations do not see because of its broader geographic sampling and temporal averaging [Forbes *et al.*, 1991].

[36] Where SABER-measured amplitudes are small, they are in good agreement with GSMW-02 predictions. This is the case for January, April, and May, and for October at Arecibo. When SABER-measured amplitudes are large, as for July and August, GSMW-02 fails to match the measurements.

[37] Seasonally, the semidiurnal phase structures measured by the lidar and SABER compare well. There are exceptions however, particularly January over Maui, when the SABER-measured phase departs substantially from the lidar-measured phase above 95 km. SABER measures very small amplitudes over Maui, so local modification of the tide is likely. In October, when the lidars observe very small tidal amplitudes, SABER observes larger amplitudes, especially over Maui, and the phase consistently leads that of the lidar by ~ 2 h. Again, local effects are likely the cause, but in this case they act counter to the semidiurnal tide. GSMW-02 semidiurnal phase results produce acceptable agreement with the observations in April, May, and with the Maui lidar

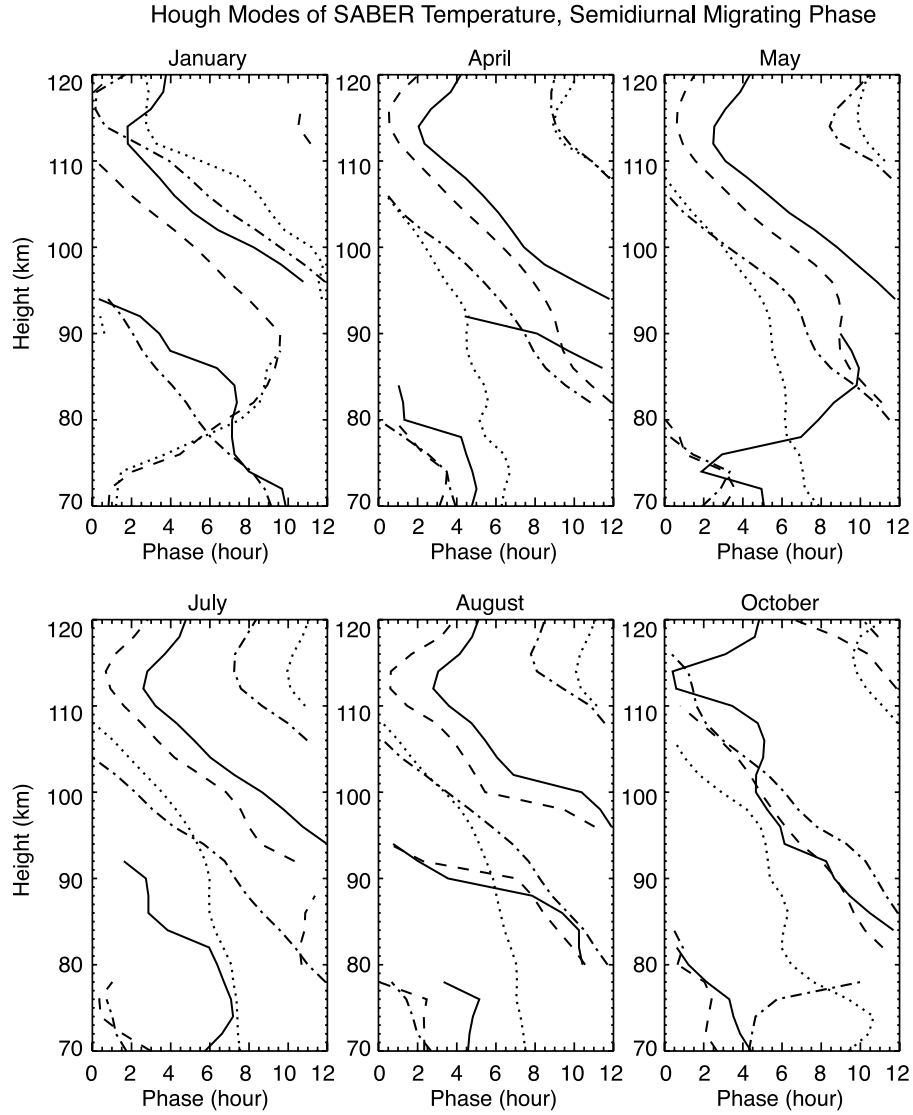


Figure 13. Phases of the semidiurnal Hough modes from SABER observations for the 6 months covered in this report. Plotted are (2, 2) (solid line), (2, 3) (dotted line), (2, 4) (dashed line), and (2, 5) (dash-dotted line).

in October. In other months, there is not good agreement, and GSWM-02-predicted phases are 180° off in the summer months, while in January they only agree with the Arecibo measurements above 95 km. Finally, the measured semidiurnal wavelength tends to be much shorter than expected from theory.

[38] A modal decomposition of the SABER data shows that the principal semidiurnal modes, dominated by (2, 2), (2, 3) and (2, 4), do have shorter than expected vertical wavelengths (Figure 13). Added to that is the fact that the (2, 2) mode and sometimes the (2, 3) mode can propagate into the lower thermosphere (Figure 12). On the basis of these results we conclude that the lower-order tidal modes are the primary contributors to the observed semidiurnal tides at Maui and Arecibo. We speculate that the winter-summer asymmetry in the semidiurnal phase structure, particularly seen at Arecibo, is the result of the importance of the asymmetrical (2, 3) mode, which is strong in summer but weak in winter.

[39] Disagreement between the lidar and SABER observations results from both sampling effects and locally driven modulations. SABER observes over a large geographical area around the ground-based sites and requires 60 days to accumulate a full diurnal cycle of data, which will smooth out locally modulated enhancements or diminutions that the lidar is sensitive to. The lidars are limited to observations within a small range of their sites and, for this report, were limited to nocturnal-only measurements, making them insensitive to the diurnal tide. Some idea of the diurnal tide could be ascertained by looking at the difference between dusk and dawn observations, but these are at most 11 h apart. Ultimately, lidar measurements must extend to daylight hours, a capability few mesospheric lidars have, and which Arecibo has only recently implemented.

[40] Extensions of these measurements would enhance our understanding of longitudinal variations in diurnal thermal structure of the MLT region. For example, lidars located at more than two sites along a given longitude

would provide greater sensitivity to the zonal variations in semidiurnal amplitude and phase reported by SABER. Full diurnal cycle measurements from the ground-based sites are ultimately vital to finally determining the influence of the diurnal tide, and multiday measurements can provide critical data on planetary waves. At the same time, high time resolution ground-based measurements (<10 min) can supply needed information on gravity wave spectra. Knowledge of local PW and GW activities will further clarify the influences that result in local modulations of the tidal structure. Finally, MLT temperature measurements that could be made by multiple passes from a high-speed long-range aircraft, such as HIAPER (<http://www.hiaper.ucar.edu/>) [Laursen et al., 2006] would permit us to see with high time and spatial resolution the localized tidal structure over regions that cannot support ground-based observations.

[41] **Acknowledgments.** The Arecibo Observatory is operated by Cornell University under a cooperative agreement with the National Science Foundation. This work is also supported by NSF grant ATM-0535457. X. Chu is supported by NSF grants ATM-0602334 and CEDAR ATM-0632501. J. Friedman acknowledges Tao “Titus” Yuan of Colorado State University for his contribution through extensive discussions of tidal theory and how to interpret the lidar results. J. Friedman and X. Chu gratefully acknowledge the thoughtful advice of Ruth Lieberman of Colorado Research Associates. J. Forbes and X. Zhang acknowledge assistance under NASA TIMED Guest Investigator Award NNX08AF22G to the University of Colorado.

References

- Chapman, S., and R. S. Lindzen (1970), *Atmospheric Tides*, Springer, New York.
- Chen, S., Z. Hu, M. A. White, H. Chen, D. A. Krueger, and C. Y. She (2000), Lidar observations of seasonal variation of diurnal mean temperature in the mesopause region over Fort Collins, Colorado (41°N, 105°W), *J. Geophys. Res.*, 105(D10), 12,371–12,379, doi:10.1029/2000JD900045.
- Chu, X., C. S. Gardner, and S. J. Franke (2005), Nocturnal thermal structure of the mesosphere and lower thermosphere region at Maui, Hawaii (20.7°N), and Starfire Optical Range, New Mexico (35°N), *J. Geophys. Res.*, 110, D09S03, doi:10.1029/2004JD004891.
- Cierpink, K. M., J. M. Forbes, S. Miyahara, Y. Miyoshi, A. Fahrutdinova, C. Jacobi, A. Manson, C. Meek, N. J. Mitchell, and Y. Portnyagin (2003), Longitude variability of the solar semidiurnal tide in the lower thermosphere through assimilation of ground- and space-based wind measurements, *J. Geophys. Res.*, 108(A5), 1202, doi:10.1029/2002JA009349.
- Dao, P. D., R. Farley, X. Tao, and C. S. Gardner (1995), Lidar observations of the temperature profile between 25 and 103 km: Evidence of strong tidal perturbation, *Geophys. Res. Lett.*, 22(20), 2825–2828, doi:10.1029/95GL02950.
- Forbes, J. M. (1995), Tidal and planetary waves, in *The Upper Mesosphere and Lower Thermosphere: A Review of Experiment and Theory*, *Geophys. Monogr. Ser.*, vol. 87, edited by R. M. Johnson and T. L. Killeen, pp. 67–87, AGU, Washington, D. C.
- Forbes, J. M., and H. B. Garrett (1978), Thermal excitation of atmospheric tides due to insolation absorption by O₃ and H₂O, *Geophys. Res. Lett.*, 5(12), 1013–1016, doi:10.1029/GL005i012p01013.
- Forbes, J. M., and H. B. Garrett (1979), Theoretical studies of atmospheric tides, *Rev. Geophys.*, 17, 1951–1981, doi:10.1029/RG017i008p01951.
- Forbes, J. M., and D. Wu (2006), Solar tides as revealed by measurements of mesospheric temperature by the MLS experiment on UARS, *J. Atmos. Sci.*, 63, 1776–1797, doi:10.1175/JAS3724.1.
- Forbes, J. M., J. Gu, and S. Miyahara (1991), On the interactions between gravity waves and the diurnal propagating tide, *Planet. Space Sci.*, 39(9), 1249–1257, doi:10.1016/0032-0633(91)90038-C.
- Forbes, J. M., M. E. Hagan, X. Zhang, and K. Hamilton (1997), Upper atmosphere tidal oscillations due to latent heat release in the tropical troposphere, *Ann. Geophys.*, 15, 1165–1175, doi:10.1007/s00585-997-1165-0.
- Forbes, J. M., J. Russell, S. Miyahara, X. Zhang, S. E. Palo, M. Mlynczak, C. J. Mertens, and M. E. Hagan (2006), Troposphere-thermosphere tidal coupling as measured by the SABER instrument on TIMED during July–September 2002, *J. Geophys. Res.*, 111, A10S06, doi:10.1029/2005JA011492.
- Forbes, J. M., X. Zhang, S. E. Palo, J. Russell, C. J. Mertens, and M. Mlynczak (2008), Tidal variability in the ionospheric dynamo region, *J. Geophys. Res.*, 113, A02310, doi:10.1029/2007JA012737.
- Fricke-Begemann, C., and J. Höffner (2005), Temperature tides and waves near the mesopause from lidar observations at two latitudes, *J. Geophys. Res.*, 110, D19103, doi:10.1029/2005JD005770.
- Friedman, J. S. (2003), Tropical mesopause climatology over the Arecibo Observatory, *Geophys. Res. Lett.*, 30(12), 1642, doi:10.1029/2003GL016966.
- Friedman, J. S., and X. Chu (2007), Nocturnal temperature structure in the mesopause region over the Arecibo Observatory (18.35°N, 66.75°W): Seasonal variations, *J. Geophys. Res.*, 112, D14107, doi:10.1029/2006JD008220.
- Hagan, M. E., and J. M. Forbes (2002), Migrating and nonmigrating semidiurnal tides in the middle and upper atmosphere excited by tropospheric latent heat release, *J. Geophys. Res.*, 107(D24), 4754, doi:10.1029/2001JD001236.
- Hagan, M. E., and J. M. Forbes (2003), Migrating and nonmigrating semidiurnal tides in the upper atmosphere excited by tropospheric latent heat release, *J. Geophys. Res.*, 108(A2), 1062, doi:10.1029/2002JA009466.
- Hecht, J. H., et al. (1998), A comparison of atmospheric tides inferred from observations at the mesopause during ALOHA-93 with the model predictions of the TIME-GCM, *J. Geophys. Res.*, 103(D6), 6307–6322, doi:10.1029/97JD03377.
- Laursen, K. K., D. P. Jorgensen, G. P. Brasseur, S. L. Ustin, and J. R. Huning (2006), HIAPER: The next generation NSF/NCAR research aircraft, *Bull. Am. Meteorol. Soc.*, 87(7), 896–909, doi:10.1175/BAMS-87-7-896.
- Mertens, C. J., et al. (2004), SABER observations of mesospheric temperatures and comparisons with falling sphere measurements taken during the 2002 summer MaCWAVE campaign, *Geophys. Res. Lett.*, 31, L03105, doi:10.1029/2003GL018605.
- Roper, R. G., G. W. Adams, and J. W. Brosnahan (1993), Tidal winds at mesopause altitudes over Arecibo (18°N, 67°W), 5–11 April 1989 (AIDA '89), *J. Atmos. Terr. Phys.*, 55, 289–312, doi:10.1016/0021-9169(93)90070-F.
- Salah, J. E., and R. H. Wand (1974), Tides in the temperature of the lower thermosphere at mid-latitudes, *J. Geophys. Res.*, 79(28), 4295–4304, doi:10.1029/JA079i028p04295.
- Salah, J. E., R. M. Johnson, and C. A. Tepley (1991), Coordinated incoherent scatter radar observations of the semidiurnal tide in the lower thermosphere, *J. Geophys. Res.*, 96(A2), 1071–1080, doi:10.1029/90JA01529.
- She, C. Y., and U. von Zahn (1998), Concept of a two-level mesopause: Support through new lidar observations, *J. Geophys. Res.*, 103(D5), 5855–5863, doi:10.1029/97JD03450.
- She, C. Y., S. Chen, B. P. Williams, Z. Hu, and D. A. Krueger (2002), Tides in the mesopause region over Fort Collins, Colorado (41°N, 105°W) based on lidar temperature observations covering full diurnal cycles, *J. Geophys. Res.*, 107(D18), 4350, doi:10.1029/2001JD001189.
- She, C. Y., T. Li, R. L. Collins, T. Yuan, B. P. Williams, T. D. Kawahara, J. D. Vance, P. E. Acott, and D. A. Krueger (2004), Tidal perturbations and variability in the mesopause region over Fort Collins, CO (40°N, 105°W): Continuous multi-day temperature and wind lidar observations, *Geophys. Res. Lett.*, 31, L24111, doi:10.1029/2004GL021165.
- States, R. J., and C. S. Gardner (1999), Structure of the mesospheric Na layer at 40°N latitude: Seasonal and diurnal variations, *J. Geophys. Res.*, 104(D9), 11,783–11,798, doi:10.1029/1999JD900002.
- States, R. J., and C. S. Gardner (2000a), Thermal structure of the mesopause region (80–105 km) at 40°N latitude. Part I: Seasonal variations, *J. Atmos. Sci.*, 57, 66–77, doi:10.1175/1520-0469(2000)057<0066:TSOTMR>2.0.CO;2.
- States, R. J., and C. S. Gardner (2000b), Thermal structure of the mesopause region (80–105 km) at 40°N latitude. Part II: Diurnal variations, *J. Atmos. Sci.*, 57, 78–92, doi:10.1175/1520-0469(2000)057<0078:TSOTMR>2.0.CO;2.
- Taylor, M. J., W. R. Pendleton, H.-L. Liu, C. Y. She, L. C. Gardner, R. G. Roble, and V. Vasoli (2001), Large amplitude perturbations in mesospheric OH Meinel and 87-km Na lidar temperatures around the autumnal equinox, *Geophys. Res. Lett.*, 28(9), 1899–1902, doi:10.1029/2000GL012682.
- Williams, B. P., C. Y. She, and R. G. Roble (1998), Seasonal climatology of the nighttime tidal perturbation of temperature in the midlatitude mesopause region, *Geophys. Res. Lett.*, 25(17), 3301–3304, doi:10.1029/98GL02558.
- Yuan, T., et al. (2006), Seasonal variation of diurnal perturbations in mesopause region temperature, zonal, and meridional winds above Fort Collins, Colorado (40.6°N, 105°W), *J. Geophys. Res.*, 111, D06103, doi:10.1029/2004JD005486.

- Yuan, T., H. Schmidt, C. Y. She, D. A. Krueger, and S. Reising (2008), Seasonal variations of semidiurnal tidal perturbations in mesopause region temperature, zonal and meridional winds above Fort Collins, CO (40.6°N , 105°W), *J. Geophys. Res.*, **113**, D20103, doi:10.1029/2007JD009687.
- Zhang, S. P., R. G. Roble, and G. G. Shepherd (2001), Tidal influence on the oxygen and hydroxyl nightglows: Wind Imaging Interferometer observations and thermosphere/ionosphere/mesosphere electrodynamics general circulation model, *J. Geophys. Res.*, **106**(A10), 21,381–21,394, doi:10.1029/2000JA000363.
- Zhang, X., J. M. Forbes, M. E. Hagan, J. M. Russell III, S. E. Palo, C. J. Mertens, and M. G. Mlynczak (2006), Monthly tidal temperatures 20–120 km from TIMED/SABER, *J. Geophys. Res.*, **111**, A10S08, doi:10.1029/2005JA011504.
- Zhao, Y., M. J. Taylor, and X. Chu (2005), Comparison of simultaneous Na lidar and mesospheric nightglow temperature measurements and the effects of tides on the emission layer heights, *J. Geophys. Res.*, **110**, D09S07, doi:10.1029/2004JD005115.
- Zhou, Q. H., M. P. Sulzer, and C. A. Tepley (1997), An analysis of tidal and planetary waves in the neutral winds and temperature observed at low-latitude *E* region heights, *J. Geophys. Res.*, **102**(A6), 11,491–11,505, doi:10.1029/97JA00440.
-
- X. Chu, CIRES, University of Colorado, Boulder, CO 80309, USA.
 J. M. Forbes and X. Zhang, Department of Aerospace Engineering Sciences, University of Colorado, Boulder, CO 80309, USA.
 J. S. Friedman, Arecibo Observatory, NAIC, P.O. Box 995, Arecibo, PR 00613-0995, USA. (jsf16@cornell.edu)